ACS Catalysis

Letter

pubs.acs.org/acscatalysis

Transient Behavior of Ni@NiO_x Functionalized $SrTiO_3$ in Overall Water Splitting

Kai Han, Tomas Kreuger, Bastian Mei, and Guido Mul*

Photocatalytic Synthesis Group, MESA+ Institute for Nanotechnology, Faculty of Science and Technology, University of Twente, Meander 229, P.O. Box 217, 7500 AE Enschede, The Netherlands

Supporting Information

ABSTRACT: Transients in the composition of Ni@NiO_x core−shell co-catalysts deposited on $SrTiO_3$ are discussed on the basis of state-of-the-art continuous analysis of photocatalytic water splitting, and post-XPS and TEM analyses. The formation of excessive hydrogen (H_2:O_2 ≫ 2) in the initial stages of illumination demonstrates oxidation of $Ni(OH)_2$ to NiOOH (nickel oxyhydroxide), with the latter catalyzing water oxidation. A disproportionation reaction of Ni and NiOOH, yielding $Ni(OH)_2$ with residual embedded Ni, occurs when illumination is discontinued, which explains repetitive transients in (excess) hydrogen and oxygen formation when illumination is reinitiated.

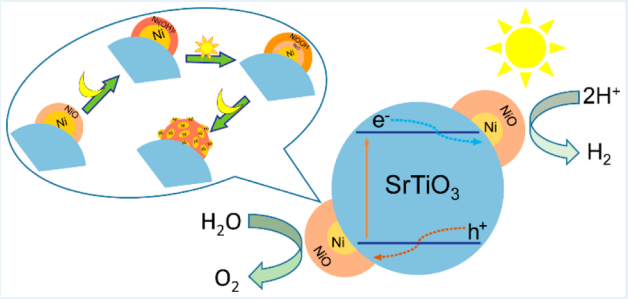

KEYWORDS: *solar water splitting, $SrTiO_3$, Ni@NiO_x co-catalysts, transient behavior, regeneration*

Research on photocatalysis for water splitting in slurry phase reactors, yielding hydrogen and oxygen, has focused on (i) doping, creating optimized semiconductors for conversion of sunlight into excited states (holes and electrons), and (ii) functionalizing (doped) semiconductor crystals with so-called co-catalyst nanoparticles to enhance the reaction rates of the necessary surface redox reactions (proton reduction and water oxidation).[1] One such co-catalyst system that has attracted significant attention is a composite of Ni@NiO_x particles. However, the structure, mode of operation, and stability of the active Ni@NiO_x particles is yet unresolved, and each appears to be dependent on the composition and structure of the semiconductor.[2−7]For strontium titanate ($SrTiO_3$), which is a semiconductor capable of inducing both half-reactions of overall water splitting, Domen et al.[2] proposed that Ni@NiO_x core−shell particles provide the catalytic sites for hydrogen evolution. In their proposal, water oxidation is catalyzed by the $SrTiO_3$ surface. More recently, Osterloh et al.[7] suggested that the core−shell model is not representing the active phase(s), but rather segregated particles of Ni and NiO_x, which promote the formation of hydrogen and oxygen, respectively.

Both Domen et al.[2] and Osterloh et al.[7] used batch reactors to evaluate catalytic performance,[2,7] which complicates evaluation of transients in hydrogen and oxygen evolution during the initial phase of water splitting. Recently, Crozier et al. reported continuous flow experiments on the use of Ni@NiO_x core−shell particles to promote activity of TiO_2 or Ta_2O_5 in overall water splitting.[5,6] During these experiments, oxygen could not be detected and a decreasing trend in hydrogen production rate was observed, which the authors explain based on the HRTEM images by oxidation and subsequent dissolution of Ni out of the Ni@NiO_x core−shell particles. Hollow NiO_x shells were observed, while Ni dissolution was substantiated by ICP analysis of the solution.[5] Besides the work of Crozier,[5,6] there has been little research into the transient behavior of functionalized semiconductors in (the initial hours of) photocatalytic activity.[8] Furthermore, transients occurring when the slurry is maintained in dark conditions (catalyst regeneration[9]), to the best of our knowledge, have never been addressed for Ni@NiO_x core−shell particles.

In this study, we describe the use of a continuously stirred tank reactor (CSTR) connected to a micro gas chromatograph equipped with a pulsed discharge detector (PDD), providing unprecedented sensitivity and data density, to analyze the transient behavior of Ni@NiO core−shell particles deposited on $SrTiO_3$ in the initial stages of water splitting, after preparation and conditioning in the darkness. We reveal significant transients in the hydrogen production rate, which correlate to changes in the composition and structure of the Ni@NiO_x core−shell particles. The implications of these transients for determination of the active phase of Ni@NiO_x core−shell particles on $SrTiO_3$, as well as the consequences for structural design, allowing practical application, are discussed.

$SrTiO_3$ was prepared according to previous reports (see the Supporting Information). As expected, X-ray diffractometry (XRD), Raman spectroscopy, and scanning electron microscopy (SEM) revealed that well-crystallized, phase-pure $SrTiO_3$ particles with an ideal cubic perovskite structure were obtained (Figures S1−S3 in the Supporting Information). Additional diffraction lines at 2θ values of 36.3° and 44.5°, characteristic

Received: December 24, 2016
Published: January 24, 2017

DOI: 10.1021/acscatal.6b03662
ACS Catal. 2017, 7, 1610−1614

for Ni and NiO_x (Figure S1), confirm the loading of well-distributed $Ni@NiO_x$ core−shell particles, as observed in the SEM images of Figure S3.

The activity of the $Ni@NiO_x$-$SrTiO_3$ (BSTO-1000-NiO_x) composite material was tested in overall water splitting under solar light illumination (see the Supporting Information) and the rates of H_2 and O_2 evolution were measured as a function of time (see Figure 1; Figure S4 in the Supporting Information shows integrated H_2 and O_2 yields).

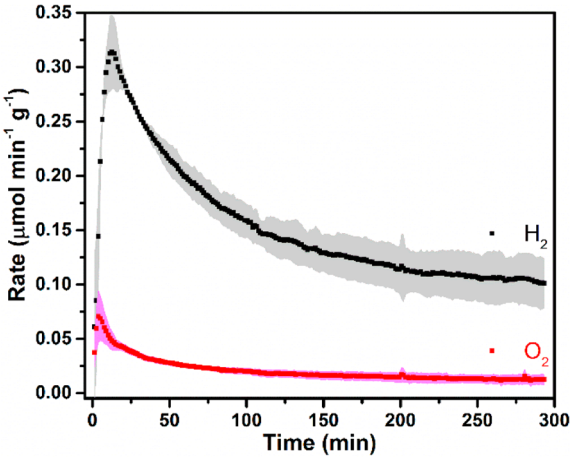

Figure 1. Transient behavior in H_2 and O_2 evolution during photocatalytic water splitting of 25 mg of BSTO-1000-NiO_x (black trace, hydrogen; red trace, oxygen). The light gray and purple areas represent the errors obtained from the standard deviation.

Immediately after starting irradiation, significant H_2 and O_2 production was observed and a maximum H_2 evolution rate of 0.3 μmol min^{-1} g^{-1} was obtained after 15 min. Both H_2 and O_2 production rate decline after reaching the maximum, with the O_2 production rate declining significantly faster and approaching apparent steady-state conditions. Based on volume and gas-flow rate, CSTR behavior would induce a fast increase in detected products,[8] whereas the slow transient behavior observed here points toward a composite material that degrades or dynamically changes during photocatalytic testing. Interestingly, significant deviation from the stoichiometric H_2:O_2 ratio of 2:1 was detected. Immediately after switching-off the light, both H_2 and O_2 evolution rapidly discontinue, confirming that H_2 and O_2 are formed in a photon-driven reaction.

To obtain further insights into the transient behavior in the initial phase of photocatalytic water splitting, variable times between illumination and dark conditions were applied. The obtained results are shown in Figure 2. The initial transients are in good agreement with the results presented in Figure 1. After purging of the reactor with pure helium for 1 h in dark conditions, a new maximum (72% of the initial maximum) in activity of H_2 evolution was obtained, when illumination was reinitiated. Consecutive dark−light cycles show that the initial H_2 evolution rate is dependent on the duration of the dark treatment. After treatment in dark conditions for 48 h, the initial H_2 evolution rate can be fully recovered, although the duration of the transient appears shorter than for the fresh catalyst. The consecutive transient again shows that ∼73% of the initial hydrogen activity can be recovered after 1 h in dark conditions. The oxygen evolution rate is significantly larger after keeping the reactor for 48 h in darkness (without reaching a maximum) than that obtained for the fresh catalyst, and at the

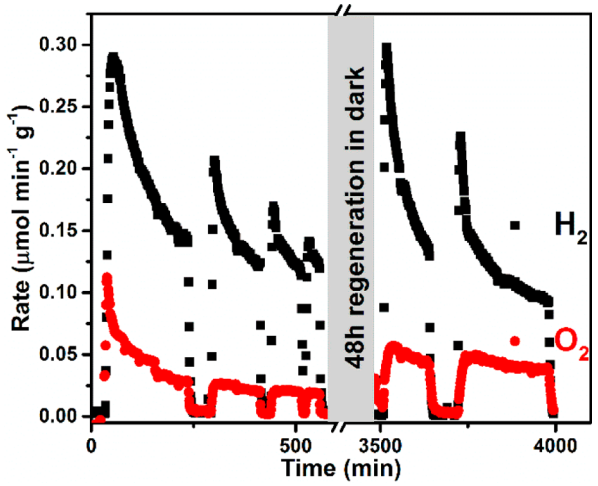

Figure 2. Transient behavior in H_2 and O_2 evolution during photocatalytic water splitting of 25 mg of BSTO-1000-NiO_x (black trace, hydrogen; red trace, oxygen).

end of the final transient, the catalyst is providing a H_2:O_2 ratio close to 2:1.

This particular behavior clearly points toward a dynamically changing co-catalyst, which has not been previously reported for $Ni@NiO_x$. $SrTiO_3$ is not changing morphology during the course of water splitting, as corroborated by HRSEM and XRD analysis after testing (see Figure S5 in the Supporting Information).

The $Ni@NiO_x$ co-catalyst was characterized after different treatments in order to explain the observed transients. The X-ray photoelectron spectra in the Ni region of the BSTO1000-NiO_x catalyst before illumination, after illumination, and after 48 h of treatment in darkness, are compared in Figure 3. For the as-prepared BSTO1000-NiO_x composite, a complex Ni peak shape is observed, evidencing that Ni is present in various oxidation states. Deconvolution of the Ni $2p_{3/2}$ signal confirms the presence of metallic Ni^0 (at 851.9 eV), Ni^{2+} (as in NiO at 853.5 eV), and Ni^{2+} (as in $Ni(OH)_2$ at 855.6 eV).[10−12] The

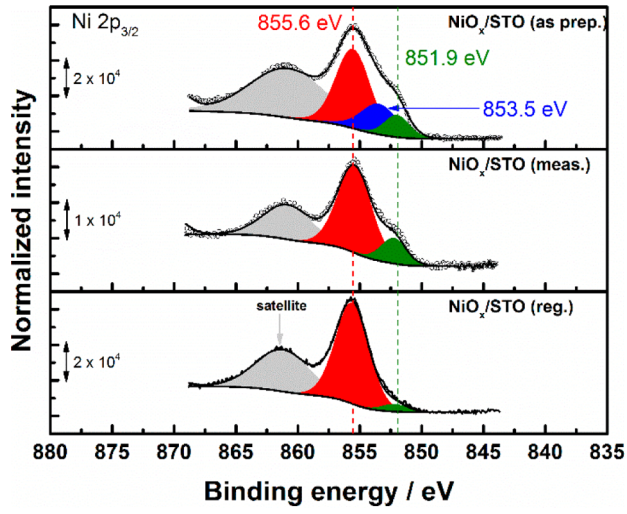

Figure 3. XPS spectra of the Ni $2p_{3/2}$ region of the BSTO1000-NiO_x sample: (i) before illumination $Ni@NiO_x$/STO (as prep.), (ii) after illumination $Ni@NiO_x$/STO (meas.), and (iii) after regeneration (48 h) $Ni@NiO_x$/STO (reg.).

DOI: 10.1021/acscatal.6b03662
ACS Catal. 2017, 7, 1610−1614

Table 1. Relative Atomic Percentages of Ni^0 and Ni^{2+}, As Determined from XPS Measurements of the Samples at Different Stages of Photocatalytic Testing[a]

sample	Ni [at.%]	Ni^0 (as metallic nickel) [%]	Ni^{2+} (as NiO) [%]	$Ni^{2+/3+}$ (as $Ni(OH)_2$/NiOOH) [%]	$Ni^0/Ni^{2+/3+}$
Ni@NiO_x/STO (as prep.)	38.8	12.3	35.2	52.5	0.2
Ni@NiO_x/STO (meas.)	21.7	17.4		82.6	0.2
Ni@NiO_x/STO (reg.)	36.0	5.7		94.3	0.06
Ni@NiO_x/STO (reg. + tested)	35.0	8.8		91.2	0.1

[a]The Ni loading (at. %) was derived from the total metal loading.

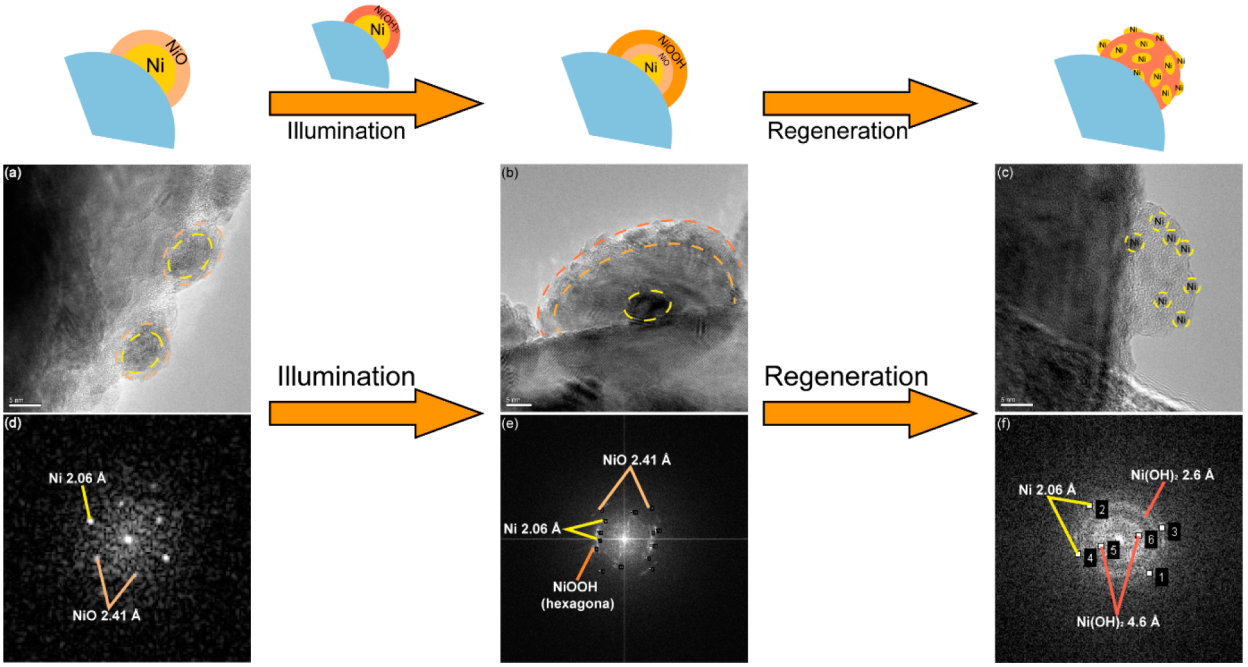

Figure 4. HRTEM images and corresponding FFT results of the (a,d) as-prepared, (b,e) illuminated, and (c,f) regenerated Ni@NiO_x $SrTiO_3$ composite material. The observed changes in morphology and composition of the Ni@NiO_x co-catalysts during overall water splitting are also schematically indicated.

derived relative percentages of Ni metal and Ni oxide, as well as the overall atomic Ni content, are shown in Table 1.

After illumination, the deconvolution of the Ni $2p_{3/2}$ region suggests that Ni is predominantly present in two different oxidation states, namely, Ni^0 and Ni^{2+} (as in $Ni(OH)_2$ at 855.6 eV). A contribution of Ni^{2+} in a NiO environment appears less likely, as the width and the symmetry of the Ni signal has clearly changed, compared to the as-prepared composite material. Moreover, it is known from studies on electrochemical oxygen evolution that NiO is not a stable phase.[13,14] These studies, and thermodynamics (see the Pourbaix diagram shown in Figure S7 in the Supporting Information), suggest that, in addition to $Ni(OH)_2$, the formation of NiOOH is feasible upon illumination.[7,15] Thus, we propose the XPS signature at higher binding energies can be assigned to a mixture of $Ni(OH)_2$ and NiOOH. Finally, the Ni atomic concentration at the surface of Ni@NiO_x/STO (meas.) decreases from 38.8 at. % to 21.7 at. %, whereas the Ni^0:$Ni^{2+/3+}$ ratio remains constant at 0.2 (see Table 1). This apparently decreasing Ni content can be explained by (i) leaching of Ni during illumination or (ii) significant particle growth. Leaching can be discarded on the basis of the elemental analysis of the solid and solution after the reaction (see Tables S1 and S2 in the Supporting Information). In addition, the particle size distributions obtained from SEM before and after the reaction suggest that the decrease in Ni atomic concentration is due to particle growth (Figure S8 in the Supporting Information).

After regeneration (Ar/dark), the intensity of the Ni signal at 855.6 is recovered (36 at. %). In addition, the contribution of metallic Ni^0 (at 851.9 eV) to the Ni signal has almost disappeared ($Ni^0/Ni^{2+/3+}$ = 0.06), pointing toward a dynamic restructuring in the darkness. Given that the contribution of metallic Ni is significantly smaller than for the sample immediately after reaction, a reaction of NiOOH with metallic Ni (in the core) to form $Ni(OH)_2$ in conditions of darkness is proposed:

$$2NiOOH + Ni + 2H_2O \rightarrow 3Ni(OH)_2 \quad (1)$$

Finally, when the regenerated sample was illuminated again (Figure S6 in the Supporting Information), the total Ni loading remained almost constant, pointing toward a stable (size) configuration of the NiO_x co-catalyst, in agreement with the now close to 2:1 ratio of H_2:O_2, in the final measurement shown in Figure 2.

To further support the results obtained by XPS, HRTEM was used (see Figure 4, as well as Figures S9 and S10 in the Supporting Information). The Ni@NiO_x particles in as-prepared BSTO1000-NiO_x(Figure 4a) clearly show the core−shell structure (in sizes of ∼8−10 nm, with a metallic Ni core of ∼6 nm), in agreement with previous reports and XPS data.[5] The corresponding *d*-spacing of the lattice fringes obtained

DOI: 10.1021/acscatal.6b03662
ACS Catal. 2017, 7, 1610−1614

from fast Fourier transformation (FFT) indicate the presence of metallic Ni(111), and NiO(220). After illumination, i.e., after the first transients shown in Figure 2, the structure maintains the core−shell morphology. However, the metallic Ni core appears smaller than in the fresh sample (Figure 4b), and the shell appears thicker and seems to be composed of two separate phases. The *d*-spacing values derived from the FFT analysis of a variety of Ni@NiO_x particles (Figure 4b, all *d*-spacings are included in Table S3 in the Supporting Information), include values of 6.7−7.7, 2.96, and 2.36 Å, which confirms the presence of NiOOH.[16] The additional *d*-spacings also indicate the presence of Ni (2.06 Å) and NiO (2.41 Å). Hence, it is reasonable to assume that the shell is composed of NiO with superpositioned NiOOH. The regenerated sample shows different morphologies (Figure 4c). Besides residual core−shell structures, a $Ni(OH)_2$ phase with small spots of larger contrast embedded in the $Ni(OH)_2$ layer is apparent, which, according to FFT analysis, likely consist of metallic Ni (see Figure S9 in the Supporting Information).

The structural changes as identified by XPS and TEM analyses are illustrated in Figure 4. In agreement with proposed structures by Domen et al.[2] and Crozier et al.,[5,6] the as-prepared co-catalyst is composed of Ni@NiO_x core−shell particles.[2,5,6] The NiO phase is transformed by humidity and in aqueous conditions to nickel hydroxide ($Ni(OH)_2$):[2]

$$NiO + H_2O \rightarrow Ni(OH)_2 \quad (2)$$

TheseNi@$Ni(OH)_2$ core−shell particles are not stable under the experimental conditions of illumination, and, very likely, the $Ni(OH)_2$ phase is oxidized by holes to NiOOH:

$$Ni(OH)_2 + h^+ \rightarrow NiOOH + H^+ \quad (3)$$

In electrochemical water oxidation, this is a well-documented process; however, for Ni@NiO_x core−shell particles on $SrTiO_3$, this reaction has not yet been considered.[13,14] Nevertheless, this reaction might explain the substoichiometric quantity of oxygen formed in the initial transients, and it is a sacrificial reaction for the highly effective formation of hydrogen in these initial stages.

Predominantly during regeneration, we propose that NiOOH disproportionates by reaction with the Ni core (reaction 1), to form $Ni(OH)_2$, as previously discussed, being in agreement with the observed differences in XPS spectra and TEM images. Indeed, in electrochemical oxygen evolution, it is reported that, at potentials below the onset for oxygen evolution (i.e., in darkness), Ni is present as $Ni(OH)_2$.[14] Reaction 1 is accompanied by vast structural rearrangement, yielding some remaining Ni that is embedded in $Ni(OH)_2$. (Re)illumination again converts $Ni(OH)_2$ to NiOOH (hence, the initial high hydrogen production rate after a dark period), and dark treatment again converts additional Ni, according to reaction 1. As a consequence of reactions 1 and 3, the metallic Ni content decreases with time (see XPS) and, eventually, only metallic Ni will be present in small quantities (Figure 4c), if any.

When in close proximity to NiOOH, Ni initially is a sacrificial electron donor (reaction 1). Our study implies that improved performance can be obtained if Ni and $Ni(OH)_2$ are deposited on separate facets of $SrTiO_3$, reaction 3 remains feasible, and reaction 1 is prevented. Osterloh et al.[7] showed that the presence of metallic Ni is indispensable for obtaining overall water splitting (catalyzing the hydrogen evolution reaction), while the required amount might be small, compared to the amount of NiO_x species, because of very favorable hydrogen evolution kinetics.[17]

The preparation of well-defined $SrTiO_3$ crystals providing anisotropic facets was recently reported by Li et al.[18] Those crystals might be suitable to further explore the transient behavior of Ni@$NiO_x$$SrTiO_3$ composite photocatalysts, and the function of the Ni compounds of various oxidation states.

In conclusion, it is proposed that transients observed upon illumination in hydrogen evolution rates, and corresponding morphological changes of Ni@NiO_x core−shell particles investigated by TEM and XPS, can be explained by *in situ* formation of NiOOH upon illumination. The metallic Ni core serves as a sacrificial agent in the water-splitting process, and during regeneration. Certainly, long-term experiments and *in situ* studies are required to further explore the dynamic behavior of Ni@NiO_x core−shell co-catalysts.

■ ASSOCIATED CONTENT

Supporting Information

The Supporting Information is available free of charge on the ACS Publications website at DOI: 10.1021/acscatal.6b03662.

Experimental methods and additional figures including XRD, Raman, and HRSEM (Figures S1−S3 and S5); H_2 and O_2 evolution data during photocatalytic water splitting (Figure S4); Pourbaix diagram of Ni (Figure S7); particle size distribution and Ni loading (Figure S8, Table S1); ICP analysis and additional XPS and TEM data (Table S2, Figures S6, S9, and S10); *d*-spacing's obtained from FFT analysis (Table S3) (PDF)

■ AUTHOR INFORMATION

Corresponding Author

*Tel.: +31-53-4893890. Fax: +31-53-4892882. E-mail: g.mul@utwente.nl.

ORCID

Bastian Mei: 0000-0002-3973-9254

Author Contributions

All authors have given approval to the final version of the manuscript.

Notes

The authors declare no competing financial interest.

■ ACKNOWLEDGMENTS

K.H. gratefully acknowledges The Chinese Science Council for financial support. Furthermore, we would like to acknowledge Gerard Kip for performing the XPS measurements, Mark Smithers and Dr. Rico Keim for performing the analysis of the samples by scanning and transmission electron microscopy, and Caroline Lievens for helping with the ICP analysis. The students of "MooiDaen" are acknowledged for stimulating discussions.

■ REFERENCES

(1) Fabian, D. M.; Hu, S.; Singh, N.; Houle, F. a; Hisatomi, T.; Domen, K.; Osterloh, F. E.; Ardo, S. *Energy Environ. Sci.* **2015**, *8*, 2825−2850.

(2) Domen, K.; Kudo, A.; Onishi, T.; Kosugi, N.; Kuroda, H. *J. Phys. Chem.* **1986**, *90*, 292−295.

(3) Zhang, Q.; Li, Z.; Wang, S.; Li, R.; Zhang, X.; Liang, Z.; Han, H.; Liao, S.; Li, C. *ACS Catal.* **2016**, *6*, 2182−2191.

(4) Wang, J.; Zhao, J.; Osterloh, F. E. *Energy Environ. Sci.* **2015**, *8*, 2970−2976.

DOI: 10.1021/acscatal.6b03662
ACS Catal. 2017, 7, 1610−1614

(5) Zhang, L.; Liu, Q.; Aoki, T.; Crozier, P. A. *J. Phys. Chem. C* **2015**, *119*, 7207−7214.
(6) Liu, Q.; Zhang, L.; Crozier, P. A. *Appl. Catal., B* **2015**, *172*−*173*, 58−64.
(7) Townsend, T. K.; Browning, N. D.; Osterloh, F. E. *Energy Environ. Sci.* **2012**, *5*, 9543.
(8) Zoontjes, M. G. C.; Han, K.; Huijben, M.; van der Wiel, W. G.; Mul, G. *Catal. Sci. Technol.* **2016**, *6*, 7793−7799.
(9) Busser, G. W.; Mei, B.; Weide, P.; Vesborg, P. C. K.; Stührenberg, K.; Bauer, M.; Huang, X.; Willinger, M.-G.; Chorkendorff, I.; Schlögl, R.; Muhler, M. *ACS Catal.* **2015**, *5*, 5530−5539.
(10) Biesinger, M. C.; Payne, B. P.; Lau, L. W. M.; Gerson, A.; Smart, R. S. C. *Surf. Interface Anal.* **2009**, *41*, 324−332.
(11) Biesinger, M. C.; Payne, B. P.; Grosvenor, A. P.; Lau, L. W. M.; Gerson, A. R.; Smart, R. S. C. *Appl. Surf. Sci.* **2011**, *257*, 2717−2730.
(12) Grosvenor, A. P.; Biesinger, M. C.; Smart, R. S. C.; McIntyre, N. S. *Surf. Sci.* **2006**, *600*, 1771−1779.
(13) Trotochaud, L.; Young, S. L.; Ranney, J. K.; Boettcher, S. W. *J. Am. Chem. Soc.* **2014**, *136*, 6744−6753.
(14) Friebel, D.; Louie, M. W.; Bajdich, M.; Sanwald, K. E.; Cai, Y.; Wise, A. M.; Cheng, M.-J.; Sokaras, D.; Weng, T.; Alonso-Mori, R.; Davis, R. C.; Bargar, J. R.; Nørskov, J. K.; Nilsson, A.; Bell, A. T. *J. Am. Chem. Soc.* **2015**, *137*, 1305−1313.
(15) Townsend, T. K.; Browning, N. D.; Osterloh, F. E. *ACS Nano* **2012**, *6*, 7420−7426.
(16) Agrawal, A.; Habibi, H. R.; Agrawal, R. K.; Cronin, J. P.; Roberts, D. M.; Caron-Popowich, R.; Lampert, C. M. *Thin Solid Films* **1992**, *221*, 239−253.
(17) Kemppainen, E.; Bodin, A.; Sebok, B.; Pedersen, T.; Seger, B.; Mei, B.; Bae, D.; Vesborg, P. C. K.; Halme, J.; Hansen, O.; Lund, P. D.; Chorkendorff, I. *Energy Environ. Sci.* **2015**, *8*, 2991−2999.
(18) Mu, L.; Zhao, Y.; Li, A.; Wang, S.; Wang, Z.; Yang, J.; Wang, Y.; Liu, T.; Chen, R.; Zhu, J.; Fan, F.; Li, R.; Li, C. *Energy Environ. Sci.* **2016**, *9*, 2463−2469.

DOI: 10.1021/acscatal.6b03662
ACS Catal. 2017, 7, 1610−1614